

Supporting Information

Highly Dispersed Pt Species Anchored onto NH₂-Ce-MOFs and Its Derived Mesoporous Catalyst for CO Oxidation

*Zeyi Guo,^a Qi You,^a Lianghao Song,^b Guoxin Sun,^b Guozhu Chen,^{*b} Cuncheng Li,^b*

*Xianfeng Yang,^c Xun Hu^d and Xuchuan Jiang^{*a}*

^aInstitute for Smart Materials & Engineering, University of Jinan, Jinan 250022, P.R.

China. E-mail: ism_jiangxc@ujn.edu.cn

^bSchool of Chemistry and Chemical Engineering, University of Jinan, Jinan 250022,

P.R. China. E-mail: chm_chengz@ujn.edu.cn

^cAnalytical and Testing Center, South China University of Technology, Guangzhou

510640, P.R. China.

^dSchool of material science and engineering, University of Jinan, Shandong province,

255022, China.

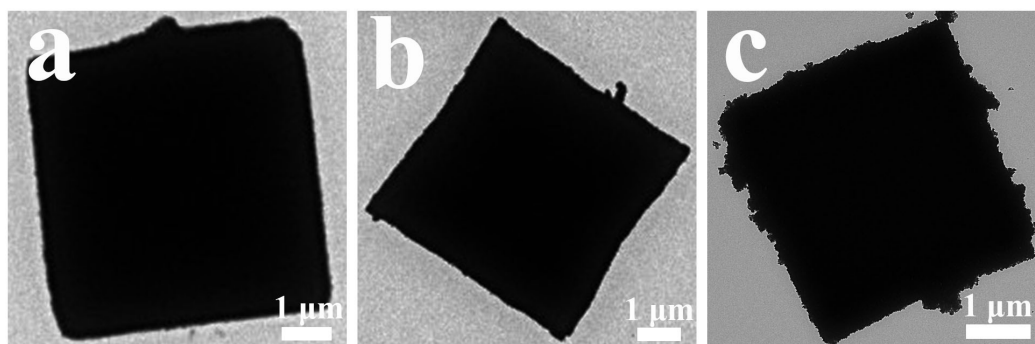


Fig. S1. TEM images of the samples: (a) $\text{NH}_2\text{-Ce-BDC}$; (b) N-Pt/CeO_2 ; and (c) IM-Pt/CeO_2 .

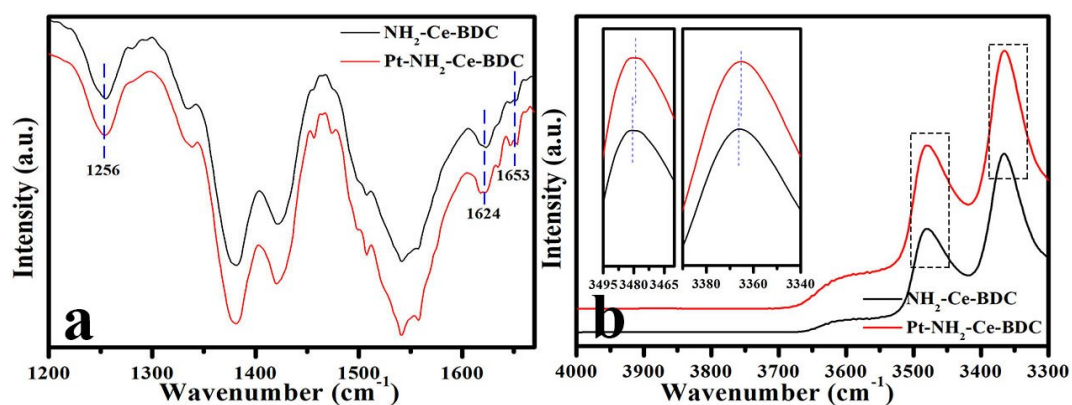


Fig. S2. (a) A partial enlarged view of Fig. 3a in the manuscript. (b) DRIFT spectra of $\text{NH}_2\text{-Ce-BDC}$ and $\text{Pt-NH}_2\text{-Ce-BDC}$. The insets are enlarged picture of the corresponding part selected by rectangle. All spectra were collected after degassing under $60 \text{ mL}\cdot\text{min}^{-1} \text{ N}_2$ flow at $150 \text{ }^\circ\text{C}$ for one hour. Totally 100 scans were accumulated for single spectrum. KBr was used as background. For comparison, all spectra were scaled by setting OCO asymmetric stretching peak ($1550\text{-}1580 \text{ cm}^{-1}$) to the same intensity.

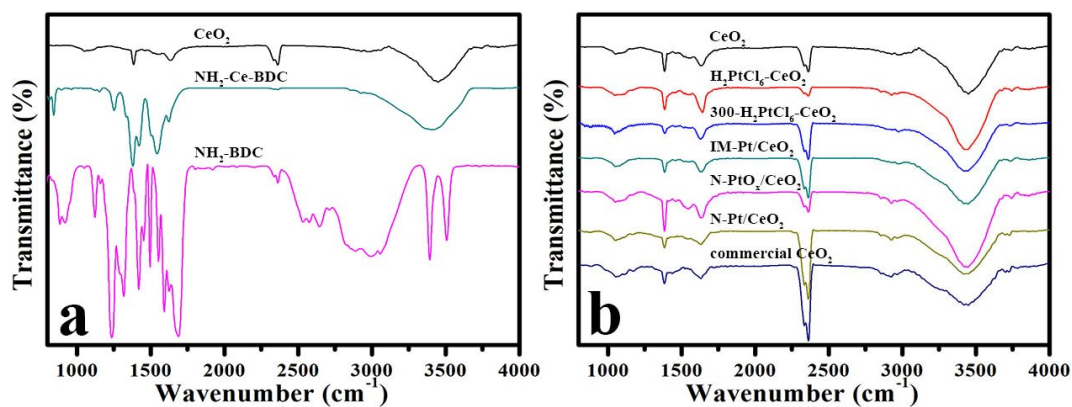


Fig. S3. FT-IR characterization of (a) the CeO_2 prepared from $\text{NH}_2\text{-Ce-BDC}$, $\text{NH}_2\text{-Ce-BDC}$ and $\text{NH}_2\text{-BDC}$; and (b) the CeO_2 , $\text{H}_2\text{PtCl}_6\text{-CeO}_2$, $300\text{-H}_2\text{PtCl}_6\text{-CeO}_2$, IM-Pt/CeO_2 , $\text{N-PtO}_x/\text{CeO}_2$, N-Pt/CeO_2 and commercial CeO_2 , respectively. (The $\text{H}_2\text{PtCl}_6\text{-CeO}_2$ sample is the sample of CeO_2 impregnated with Pt. The $300\text{-H}_2\text{PtCl}_6\text{-CeO}_2$ sample is the sample of $\text{H}_2\text{PtCl}_6\text{-CeO}_2$ after calcination at $300\text{ }^\circ\text{C}$. The $\text{N-PtO}_x/\text{CeO}_2$ sample is the sample of N-Pt/CeO_2 without reduction.)

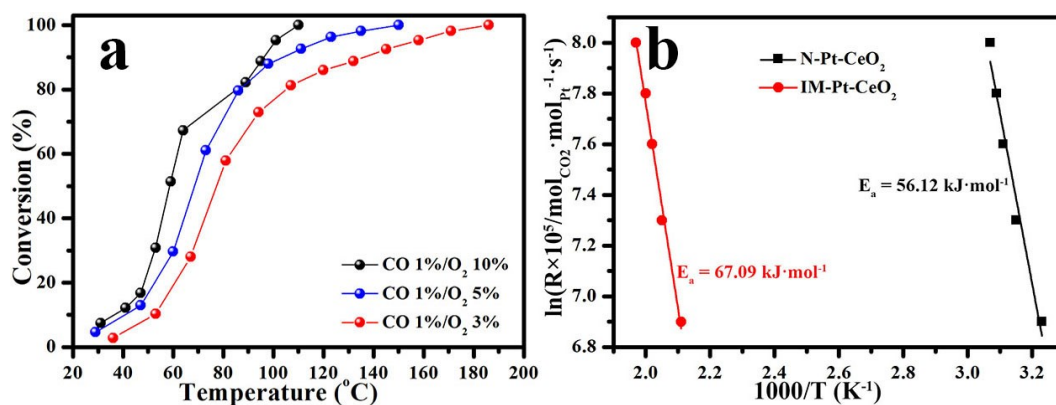


Fig. S4. (a) The catalytic performance of N-Pt/CeO₂ catalyst for CO oxidation under different O₂ concentrations. (b) Arrhenius plots for N-Pt/CeO₂ and IM-Pt/CeO₂ samples of CO reaction rates under CO conversion between 10 and 30%. Conversions of CO to CO₂ were calculated from the data (X_{CO}) from the online infrared gas analyzer for CO according to $X_{CO} = (1 - A_{CO} / A_{CO^*}) \times 100$ (%), where A_{CO^*} and A_{CO} are the data of CO before and after the reaction, respectively. The reaction rate (R , (mol of CO)·(mol of Pt)⁻¹·s⁻¹) was calculated as follows: $R = X_{CO} \times F_{CO} / M_{Pt}$. F_{CO} (mol·s⁻¹) is the flow rate of CO in reactant gas, and M_{Pt} is the amount of Pt (mol) in the used catalyst (50 mg).

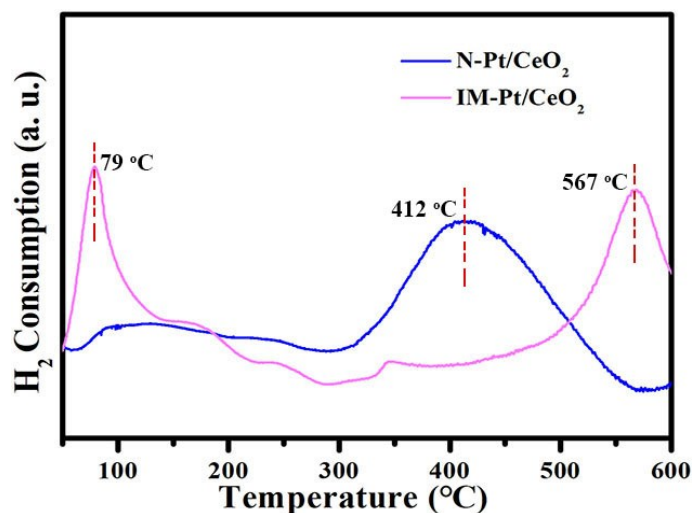


Fig. S5. Hydrogen temperature-programmed reduction (H_2 -TPR) profiles of N-Pt/CeO₂ and IM-Pt/CeO₂ samples. H_2 -TPR experiment was carried out with a thermal conductivity detector on 100 mg sample in a gas mixture (80% (molar) argon and 20% (molar) hydrogen, gas flow rate of 30 mL•min⁻¹), using a temperature ramp rate of 10 °C•min⁻¹.

As shown in Fig. S5, the peak at 79 °C in IM-Pt/CeO₂ catalyst is indexed to regenerative Pt oxide species,^[S1] while there is almost no reduction peaks in N-Pt/CeO₂ before 300 °C. The re-oxidized phenomenon is due to the small sized Pt (<3.5 nm) in IM-Pt/CeO₂, although which is larger than that of N-Pt/CeO₂. Compared with IM-Pt/CeO₂, there is a strong interaction between Pt and CeO₂ in N-Pt/CeO₂, and the resultant formation of Pt-O-Ce strong bond (refer to Raman spectra) is possibly responsible for making Pt²⁺ species difficult to be reduced.

Table S1. Comparison of this work with reported work.

Catalyst	WHSV (mL·g ⁻¹ ·h ⁻¹)	Pt loading (wt%)	T ₁₀₀ (°C)	Rates (mol _{CO} ·mol _{Pt} ⁻¹ ·s ⁻¹)	Activation energy (E _a) (kJ·mol ⁻¹)	Reference
N-Pt/CeO ₂	60000	1.33	110	0.0936 (100 °C)	56.1	This study
S-Pt/CeO ₂	72000	0.256	~140	<0.09 (100 °C)	Not stated	[S2]
R-Pt/CeO ₂	72000	0.257	~150	~0.05 (100 °C)	Not stated	[S2]
C-Pt/CeO ₂	72000	0.255	~150	~0.05 (100 °C)	Not stated	[S2]
Pt/CeO ₂ IWI	-	1.00	~250	0.0033 (110 °C)	68.0 ± 1.6	[S3]
Pt/CeO ₂ ODH-N	-	1.06	~250	0.0060 (110 °C)	56.7 ± 0.4	[S3]
Pt/CeO ₂ Gly-N	-	1.14	~200	0.0250 (110 °C)	58.8 ± 1.0	[S3]
Pt/CeO ₂ Rod	-	-	-	Not stated	101.7	[S4]
Pt/CeO ₂ Octahedra	-	-	-	Not stated	145.2	[S4]
Pt/CeO ₂ - Fecralloy foam	17000	-	>270	Not stated	~116	[S5]
Pt/CeO ₂	80000	~1.60	>155	Not stated	Not stated	[S6]
Pt/CeO ₂	-	0.98	~260	Not stated	59.0 ± 1.0	[S7]
Pt/CeO ₂	-	2.00	>270	Not stated	Not stated	[S8]
Pt/CeO ₂ Rod	-	5.00	160	0.0135 (80 °C)	34.0 ± 2.0	[S9]
Pt/CeO ₂ Cube	-	5.00	180	0.0118 (80 °C)	46.0 ± 2.0	[S9]
Pt/CeO ₂ Octahedra	-	5.00	190	0.0031 (80 °C)	63.0 ± 4.0	[S9]

Reference

- S1. M. Sun, J. Liu, C. Song, Y. Ogata, H. Rao, X. Zhao, H. Xu and Y. Chen, *ACS Appl. Mater. Interfaces*, 2019, **11**, 23102-23111.
- S2. A. Zhou, J. Wang, H. Wang, H. Li, J. Wang and M. Shen, *J. Rare Earth.*, 2018, **36**, 257-264.
- S3. F. Morfin, T.-S. Nguyen, J.-L. Rousset and L. Piccolo, *Appl. Catal. B-Environ.*, 2016, **197**, 2-13.
- S4. F. Lin, D. T. Hoang, C.-K. Tsung, W. Huang, S. H.-Y. Lo, J. B. Wood, H. Wang, J. Tang and P. Yang, *Nano Res.*, 2011, **4**, 61-71.
- S5. S. Cimino, L. Lisi, G. Totarella, S. Barison, M. Musiani and E. Verlato, *J. Ind. Eng. Chem.*, 2018, **66**, 404-410.
- S6. K. Wu, L. Zhou, C.-J. Jia, L.-D. Sun and C.-H. Yan, *Mater. Chem. Front.*, 2017, **1**, 1754-1763.
- S7. T.-S. Nguyen, F. Morfin, M. Aouine, F. Bosselet, J.-L. Rousset and L. Piccolo, *Catal. Today*, 2015, **253**, 106-114.
- S8. M. Shen, L. Lv, J. Wang, J. Zhu, Y. Huang and J. Wang, *Chem. Eng. J.*, 2014, **255**, 40-48.
- S9. N. Singhania, E. A. Anumol, N. Ravishankar and G. Madras, *Dalton Trans.*, 2013, **42**, 15343-15354.